


## THE INFLUENCE OF INTERACTIONS OF DISTANT GALAXIES ON THEIR NON-THERMAL RADIO EMISSION

MARINA S. PAVLOVIĆ<sup>1</sup>  and TIJANA PRODANOVIĆ<sup>2</sup> 

<sup>1</sup>*Mathematical Institute of the Serbian Academy of Sciences and Arts,  
Kneza Mihaila 36, 11000 Belgrade, Serbia*

<sup>2</sup>*Department of Astronomy, Faculty of Mathematics,  
Studentski trg 16, 11000 Belgrade, Serbia  
E-mail: marinap@mi.sanu.ac.rs*

**Abstract.** It has been established that a strong linear correlation exists between the thermal far-infrared (FIR) and non-thermal radio emissions of star-forming galaxies. Recent research on this correlation at high redshifts has revealed that it is evolving as redshifts increase. This paper explores potential physical factors contributing to this correlation's evolution, with one likely explanation being galaxy interactions. To investigate this hypothesis, a sample of dusty star-forming galaxies from the COSMOS field, up to a redshift of  $z = 3.5$ , was carefully selected. The sample was divided into two subsets based on morphological types: disk and irregular galaxies. Here we use galactic morphology as an indicator of past or ongoing interactions, as irregular galaxy shapes are often the result of collisions or close encounters. The evolution of the correlation with redshift was analyzed separately for each subset. This study lack of indication of redshift evolution in the FIR-radio correlation for both disk and irregular galaxy subsets. However, the analysis did reveal a hint that irregular galaxies exhibited a lower mean correlation parameter,  $q_{\text{FIR}}$ , suggesting that they might influence the correlation's evolution if their prevalence in the sample increases at higher redshifts.

### 1. INTRODUCTION

Observations have revealed a strong connection between radio and far-infrared emissions in star-forming galaxies, called the Far-infrared radio correlation (FIRC) (Yun et al. 2001, Algera et al. 2020). This correlation likely arises from the life cycle of massive stars, as young, massive stars serve as the primary heat source for interstellar dust, leading to thermal infrared emissions. After these stars explode as supernovae, their remnants accelerate cosmic rays, generating non-thermal radiation. The FIRC's stability has made it valuable in astrophysics, helping in the identification of radio-loud active galactic nuclei (AGNs) (Del Moro et al. 2013), distance estimations for high-redshift galaxies (Murphy et al. 2012), and as a tool for estimating the Star Formation Rate (SFR) using radio luminosity (Murphy et al. 2012).

The FIRC is characterized by the ratio parameter  $q_{\text{FIR}} = \log \left( \frac{F_{\text{FIR}}}{3.75 \times 10^{12} \text{Wm}^{-2}} \right) - \log \left( \frac{S_{1.4}}{\text{Wm}^{-2}\text{Hz}^{-1}} \right)$ , where  $S_{1.4}$ , represent the rest-frame radio emission flux density at 1.4 GHz, and  $F_{\text{FIR}}$  represent the rest-frame far-infrared emission flux density spanning from  $42\mu\text{m}$  to  $122\mu\text{m}$  (Helou et al. 1985). Local universe observations of star-forming galaxies established that this parameter's value is  $q_{\text{FIR},0} = 2.34 \pm 0.01$  (Yun et al. 2001). However, recent observations of 12,000 star-forming galaxies up to redshift  $z < 6$  in the COSMOS field have revealed that this parameter varies with redshift,

specifically, it decreases with redshift as  $q_{\text{FIR}}(z) = (2.52 \pm 0.03)(1+z)^{(-0.21 \pm 0.01)}$  (Delhaize et al. 2017).

Various factors have been proposed to account for the FIRC evolution with redshift. The foremost one is the influence of active galactic nuclei (Sajina et al. 2008), as there are no conclusive criteria to exclude their presence at higher redshifts. Another consideration is the possible impact of major mergers at higher redshifts (Pavlović and Prodanović 2019, Pavlović 2021). Notably, the rate of galactic mergers increases up to a redshift of approximately  $z \approx 2 - 3$  (Ventou et al. 2017). Previous studies have indicated that major mergers between galaxies can lead to an enhancement in non-thermal radio emission through additional synchrotron emission from gas bridges in taffy-like systems (Murphy 2013), magnetic field amplification, or the acceleration of cosmic rays in tidal shocks within the interstellar medium of interacting galaxies (Donevski and Prodanović 2015).

In our earlier study (Pavlović and Prodanović 2019), theoretical models of the FIR-radio correlation evolution with redshift were presented, with a focus on the contribution of so-called peculiar (irregular and interacting) galaxies and interacting galaxies separately (as illustrated in Figures 1 and 2 in this paper). The models in Pavlović and Prodanović (2019) show a declining correlation parameter with increasing redshift, consistent with what was found by Delhaize et al. (2017). Molnár et al. (2018) recently explored the impact of galactic morphology on the evolution of the FIRC up to a redshift of approximately  $z \approx 1.5$ . They found that in spheroid-dominant galaxies, there is a decline in the correlation parameter with redshift. In contrast, for disk-dominant galaxies, encompassing spiral/disk and irregular galaxies, the correlation's evolution is minimal. Inspired by these results, we chose to investigate the redshift-dependent evolution of the FIR-radio correlation in a larger sample of submillimeter galaxies (SMGs) taken from the COSMOS field.

## 2. SAMPLE CHARACTERIZATION

To investigate the evolution of the FIR-radio correlation, we utilized a sample of submillimeter galaxies within the  $2\text{deg}^2$  COSMOS field. The COSMOS field is covered by several morphological catalogs, including the Tasca, Cassata, and Zurich catalogs (Tasca et al. 2009, Cassata et al. 2007, Scarlata et al. 2007, Sargent et al. 2007), which were used in this study. Each of these catalogs offers a detailed morphological classification for galaxies, categorizing them into three types: 1) early type, 2) disk (spiral), and 3) irregular galaxies. The sample was first cleaned by excluding all galaxies classified as early type. To determine the morphological type for each of the selected sources, a ladder approach was used. If a source was classified as irregular/disk in all three catalogs, it was categorized as irregular/disk. When two out of the three catalogs provided the same morphology, the most commonly occurring class was adopted.

Spectroscopic redshifts were obtained from the COSMOS spectroscopic redshift master catalog (Salvato et al. in prep). These spectroscopic redshifts are highly reliable and consequently, the decision was made to utilize spectroscopic redshifts whenever available, which was the case for 33 disk galaxies and 11 irregular galaxies from our cleaned COSMOS sample. For the cases where spectroscopic redshifts were unavailable, photometric redshifts from the COSMOS2015 photometric redshift catalog (Laigle et al. 2016) were employed.

Active galactic nuclei exhibit distinct non-thermal radio emissions, which could significantly affect the evolution of the Far-infrared radio correlation and contaminate the sample. To clear the sample of AGNs, the COSMOS VLA 3GHz AGN Catalog (Smolčić et al. 2017a) was employed. We cross-referenced our sample with the COSMOS VLA 3GHz AGN Catalog and excluded any object that exhibited AGN characteristics according to any of the criteria. While this approach ensures the absence of AGN contamination in the sample, there remains a possibility of also removing star-forming sources with excess radio emission but lacking AGN characteristics. This may result in a reduction of our sample.

To calculate the total Far-infrared flux density, we used infrared observations from  $24\mu\text{m}$ ,  $100\mu\text{m}$ ,  $160\mu\text{m}$ ,  $250\mu\text{m}$ ,  $350\mu\text{m}$ , and  $500\mu\text{m}$ . These data were obtained from the Herschel continuum observations (Pilbratt et al. 2010). For each galaxy, a spectral energy distribution (SED) curve was fitted using a second-degree polynomial. Subsequently, the total FIR flux density was computed by integrating the SED curve in the galaxy’s rest frame within the range of  $42\mu\text{m}$  to  $122\mu\text{m}$ . In the radio domain, we employed the 3 GHz integrated radio flux density data from the COSMOS VLA 3GHz Multiwavelength Counterpart Catalog (Smolčić et al. 2017b) and the 1.4 GHz radio flux density from the COSMOS VLA Deep Catalog (Aretxaga et al. 2011). For galaxies with available flux data at 1.4 GHz, we computed the rest-frame, k-corrected flux densities using a previously determined spectral index (Magnelli et al. 2015) at 1.4 GHz. For the remaining galaxies in the sample, we converted the observer-frame 3 GHz flux densities into 1.4 GHz luminosities using the relation:  $L_{1.4\text{GHz}} = \frac{4\pi D_L^2}{(1+z)^{\alpha+1}} \left(\frac{1.4}{3}\right)^\alpha S_{3\text{GHz}}$ . Here the  $D_L$  is the luminosity distance to the object in meters.  $L_{1.4\text{GHz}}$  and  $S_{3\text{GHz}}$  represent the observed radio luminosity at 1.4 GHz and the observed flux density at 3 GHz, respectively and  $\alpha$  represents radio spectral index. The spectral index was calculated assuming a power-law spectrum with index  $\alpha$  where  $S_\nu \propto \nu^\alpha$  of radio sources by comparing the 3 GHz fluxes to those in the 1.4 GHz. In situations where we lack flux densities at two wavelengths in the radio domain, a fixed value of this parameter was utilized ie.  $\alpha = -0.56 \pm 0.20$  (Klein et al. 2018).

After categorizing by morphology, eliminating AGNs, and cleaning the sample, the final dataset includes 181 disk galaxies and 55 irregular galaxies.

### 3. RESULTS

To facilitate a comparison with our previous work (Pavlović and Prodanović 2019), in which we encountered a shortage of galaxies at redshifts  $z < 1$ , we analyzed the complete sample spanning the redshift range  $0 < z < 3.5$  and on a subsample with  $z > 1$ . For the entire galaxy sample, we computed the mean value of the correlation parameter to be  $q_{\text{FIR}} = 2.34 \pm 0.30$ . In the subset of galaxies with redshifts  $z > 1$ , the mean correlation parameter was determined to be  $q_{\text{FIR}}(z > 1) = 2.21 \pm 0.36$ . Furthermore, we separately calculated the mean correlation parameter for each of the subsamples, resulting in  $q_{\text{FIR}} = 2.34 \pm 0.31$  for disk galaxies and  $q_{\text{FIR}} = 2.19 \pm 0.34$  for irregular galaxies, respectively (Pavlović 2021). There is a hint that the mean  $q_{\text{FIR}}$  parameter exhibits lower values in the sample of irregular galaxies. This alignment supports the possibility that galactic collisions could be influencing the evolution of  $q_{\text{FIR}}$  towards higher redshifts.

To enable comparisons with previous studies (Delhaize et al. 2017, Pavlović et al. 2019), we investigated the relationship between the correlation parameter and redshift in the form of  $q_{\text{FIR}}(z) = a(1+z)^b$ , with  $a$  representing a fitting constant and  $b$  serving as the degree coefficient. This analysis was performed separately for two distinct morphological types. Figure 1 displays the dependency of  $q_{\text{FIR}}(z)$  as defined earlier for 181 disk galaxies (left) and 55 irregular galaxies (right). The red dashed and dash-dotted lines represent power-law fits of  $q_{\text{FIR}} = (2.4 \pm 0.01)(1+z)^{(-0.05 \pm 0.04)}$  and  $q_{\text{FIR}} = (2.2 \pm 0.1)(1+z)^{(0.04 \pm 0.08)}$  for disk and irregular galaxies, respectively. Blue lines represent the results from Molnar et al. (2018) for spheroid-dominated (left) and disk-dominated (right) galaxies for the sake of comparison. This figure is taken from the paper Pavlović (2021). When the sample of galaxies was cleaned from outliers using the 3 sigma detection we also didn't see any significant evolution of the FIR correlation with redshift. In this case, the final sample consisted of 53 irregular galaxies and 177 disk galaxies. The results in this case show dependencies  $q_{\text{FIR}} = (2.4 \pm 0.04)(1+z)^{(-0.05 \pm 0.03)}$  and  $q_{\text{FIR}} = (2.16 \pm 0.1)(1+z)^{(0.02 \pm 0.06)}$  for disk and irregular galaxies, respectively.

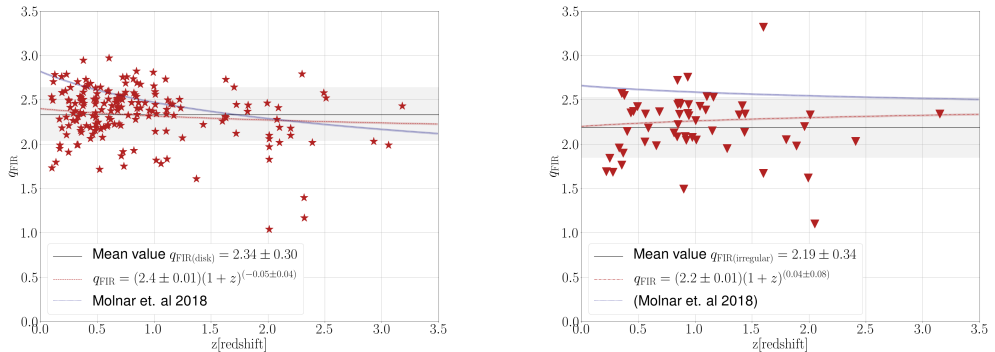


Figure 1: The graph illustrates the variation of  $q_{\text{FIR}}$  as a function of redshift. On the left side, the data for disk galaxies is denoted by red stars and fitted with the red dashed line. On the right side, data for irregular SMGs is represented by red triangles and fitted with a red dash-dotted line. The solid black line represents the mean value of the  $q_{\text{FIR}}$  parameter, with the gray-shaded region indicating its standard deviation for disk galaxies on the left and irregular galaxies on the right. Blue lines depict the results from Molnar et al. (2018) for spheroid-dominated galaxies on the left and disk-dominated galaxies on the right, serving as a basis for comparison (Pavlović 2021).

While it may appear that trends in different morphological types are differing, both are consistent within the margin of error with no detectable evolution with redshift. Nonetheless, it's important to note that limited statistics and substantial uncertainties, particularly at redshifts  $z > 1$ , may obscure any underlying evolution observed by Delhaize et al. (2017). Another potential explanation for the variation in our results compared to Delhaize et al. (2017) is the proposition that the observed evolution of the FIR-radio correlation with redshift does not exist and may instead be the consequence of an inadequate estimation of the radio spectral index in star-forming galaxies in the early universe.

Additionally, we performed an analysis of the correlation parameter's dependency on redshift for the entire sample, which includes both disk (red stars) and irregular galaxies (green triangles), counting 236 galaxies (this result can also be seen in Pavlović 2021). The fitting results are presented in Figure 2. The solid blue line in the graph represents a power-law fit for the entire sample of 236 galaxies, expressed as  $q_{\text{FIR}} = (2.4 \pm 0.01)(1 + z)^{(-0.02 \pm 0.03)}$ . The data from the entire sample does not exhibit any indications of redshift-dependent evolution. Figure 2 also includes the previously observed trend found by Delhaize et al. (2017), illustrated as an orange dotted line, allowing for easy comparison.

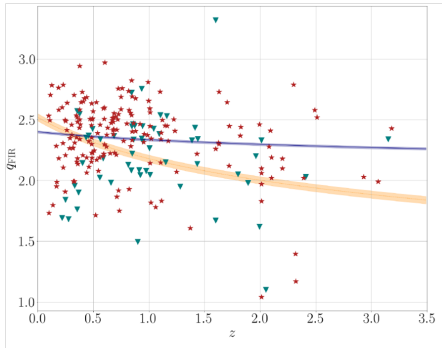


Figure 2: The graph displays  $q_{\text{FIR}}$  as a function of redshift for 236 SMGs. In the graph, red stars correspond to disk galaxies, while green triangles represent irregular galaxies. The blue solid curve illustrates a power-law fit for the entire sample of 236 SMGs, containing both disk and irregular galaxies. The orange-dotted curve represents the identical power-law fit found by Delhaize et al. (2017) for comparison.

As shown in Figure 2, the number of data points in the highest redshift bin is notably lower compared to the lower redshift bins. This difference could imply that the limited data points in these high-redshift bins may not fully represent the true value of the correlation parameter during those redshifts.

#### 4. SUMMARY

Empirically established correlations have proven to be invaluable tools for investigating galaxies at high redshifts, and this includes the Far-Infrared Radio Correlation. However, recent observations of star-forming galaxies up to redshift  $z < 6$  have unveiled an evolving trend in this correlation with redshift, described as  $q_{\text{FIR}}(z) = (2.52 \pm 0.03)(1 + z)^{(-0.21 \pm 0.01)}$  (Delhaize et al. 2017).

Building upon Pavlović et al. (2019), this study expands on galactic interaction's link with the redshift evolution of FIR correlation using a larger COSMOS survey sample of 236 star-forming galaxies (181 disks, 55 irregulars). Contrary to previous findings by Delhaize et al. (2017) and Molnar et al. (2018), we found a hint that neither disk nor irregular subsets show significant evolution of the correlation with redshift, even in the case when we remove the outliers. Irregular galaxies exhibit hint of a lower mean correlation parameter value compared to disks, partially aligning with earlier work (Pavlović et al. 2019). This hints at possible morphological influences on

the evolution of the FIR correlation. However, the reliability of optical image-based galaxy morphology parameters diminishes beyond redshift  $z > 1$ , impacting results. Thus, a key objective is to identify more precise parameters for characterizing galaxy collision stages at higher redshifts.

Lastly, it's crucial to acknowledge that the parameter  $q_{\text{FIR}}$ , which varies as  $q_{\text{FIR}} \sim (1+z)^\alpha$ , is highly sensitive to the radio spectral index (Pavlović 2021). There is a possibility that this parameter or the constant value assigned to it could be responsible for the apparent correlation evolution. This aspect will be the subject of further investigation in subsequent work.

### Acknowledgements

We would like to express our gratitude to the reviewer whose advice greatly improved this paper. This work was supported by the Ministry of Science, Technological Development and Innovation of the Republic of Serbia (contract no. 451-03-66/2024-03).

### References

- Algera, H. S. B., Smail, I., Dudzevici ut e, U., et al.: 2020, *The Astrophysical Journal*, **903**, 138
- Aretxaga, I., Wilson, G. W., Aguilar, E., et al.: 2011, *Monthly Notices of the Royal Astronomical Society*, **415**, 415
- Del Moro, A., Alexander, D. M., Mullaney, J. R., et al.: 2013, *Astronomy and Astrophysics*, **549**, A59
- Delhaize, J., Smolčić, V., Delvecchio, I., et al.: 2017, *Astronomy and Astrophysics*, **602**, A4
- Delvecchio, I., Smolčić, V., Zamorani, G., et al.: 2017, *Astronomy and Astrophysics*, **602**, A3
- Donevski, D. and Prodanović, T.: 2015, *Monthly Notices of the Royal Astronomical Society*, **453**, 638
- Helou, G., Soifer, B. T., and Rowan-Robinson, M.: 1985, *The Astrophysical Journal Letters*, **298**, L7
- Magnelli, B., Ivison, R. J., Lutz, D., et al.: 2015, *Astronomy and Astrophysics*, **573**, A45
- Molnar, D. C., Sargent, M. T., Delhaize, J., et al.: 2018, *Monthly Notices of the Royal Astronomical Society*, **475**, 827
- Murphy, E. J., Bremseth, J., Mason, B. S., et al.: 2012, *The Astrophysical Journal*, **761**, 97
- Murphy, E. J.: 2013, *The Astrophysical Journal*, **777**, 5
- Park, S. Q., Barmby, P., Fazio, G. G., et al.: 2008, *The Astrophysical Journal*, **678**, 744
- Pavlović, M., and Prodanović, T.: 2019, *Monthly Notices of the Royal Astronomical Society*, **489**, 4557
- Pavlović, M.: 2021, *Serbian Astronomical Journal*, **203**, 15
- Pilbratt, G. L., Riedinger, J. R., Passvogel, T., et al.: 2010, *Astronomy and Astrophysics*, **518**, L1
- Sajina, A., Yan, L., Lutz, D., et al.: 2008, *The Astrophysical Journal*, **683**, 65
- Sargent, M. T., Carollo, C. M., Lilly, S. J., et al.: 2007, *The Astrophysical Journal Supplement*, **172**, 434
- Scarlata, C., Carollo, C. M., Lilly, S., et al.: 2007, *The Astrophysical Journal Supplement*, **172**, 406
- Smolčić, V., Delvecchio, I., Zamorani, G., et al.: 2017a, *Astronomy and Astrophysics*, **602**, A2
- Smolčić, V., Novak, M., Bondi, M., et al.: 2017b, *Astronomy and Astrophysics*, **602**, A1
- Tasca, L. A. M., Kneib, J. P., Iovino, A., et al.: 2009, *Astronomy and Astrophysics*, **503**, 379
- Ventou, E., Contini, T., Bouche, N., et al.: 2017, *Astronomy and Astrophysics*, **608**, A9
- Yun, M. S., Reddy, N. A., and Condon, J. J.: 2001, *The Astrophysical Journal*, **554**, 803